



Colorful opaque photovoltaic modules with down-converting InP/ZnSe_xS_{1-x} quantum dot layers

Byeong Guk Jeong^{a,1}, Donghyo Hahm^{a,1}, Jeong Woo Park^a, Jun Young Kim^b, Hee-Eun Song^c, Min Gu Kang^c, Sohee Jeong^d, Gihwan Kang^{c,**}, Wan Ki Bae^{a,***}, Hyung-Jun Song^{e,*}

^a SKKU Advanced Institute of Nanotechnology (SAINT), School of Nano Science & Technology, Sungkyunkwan University, Suwon, 16419, South Korea

^b Department of Semiconductor Engineering, Gyeongsang National University, Jinju, Gyeongnam, 52828, South Korea

^c Photovoltaic Laboratory, Korea Institute of Energy Research, Daejeon, 34129, South Korea

^d Department of Energy Science, Center for Artificial Atoms, Sungkyunkwan University, Suwon, 16419, South Korea

^e Department of Safety Engineering, Seoul National University of Science and Technology, Seoul, 01811, South Korea

ARTICLE INFO

Keywords:

III-V quantum Dots
Photovoltaic (PV) module
Colored PV module
Angular independence
Ligand exchange

ABSTRACT

The luminescent down-shifting (LDS) layer, which transforms incoming high energy solar photons to visible ones, promises augmentation of both photoelectric performance and aesthetic appeals of photovoltaic (PV) modules. For efficient, colored PVs with LDS layer, luminophores with high photoluminescence quantum yield (PL QY), small overlap between absorption and emission spectra, and proven photostability are prerequisites. Here, we demonstrate colorful, opaque PV modules with LDS layers of minimized photon sacrifice enabled by structurally-engineered, eco-friendly InP/ZnSe_xS_{1-x} quantum dots (QDs). Specifically, composition-controlled, thick shells allow enhanced absorption in the UV region and improved PL QY of QDs. Additionally, the ligand-engineering guarantees the stability of LDS layers after the damp heat test. Benefited from QD-LDS layers, commercially available CIGS and c-Si PV modules are awarded with 40% EQE enhancement in the ultraviolet region and wide-ranging color tunability over the entire visible region by QD-LDS layers. Hence, this integrated approach for desirable luminophores will contribute to the realization of highly-efficient, aesthetically-appealing opaque PV modules.

1. Introduction

Photovoltaic (PV) cells and modules, which utilize the abundant sunlight arriving at the Earth's surface to generate electricity, have been considered as one of the most attractive renewable technologies due to their easiness of installation and cost competitive advantage. The accumulated capacity of PV modules exceeded 500 GW in 2019 and it is expected to continue to grow over 5 TW within the next 10 years [1,2]. Recently, growing demands to realize zero-energy buildings and sustainable cities shift gears and expedite the installation of PV modules in an urban area in familiarized forms, for instance, building integrated photovoltaics (BIPVs), energy generating windows, and portable device integrated systems [3–9].

For practicable use of building or other device integrated PV

modules, the system should be efficient in generating enough power for the self-sufficing energy consumption of buildings or devices and be durable against harsh outdoor conditions. In these respects, crystalline silicon (c-Si) and thin film (CdTe, CIGS) PV modules, which hold high power conversion efficiency (PCE, ~20%), proven operational stability (less than 20% of efficiency degradation for 20 years from installation) and cost efficiency (<\$ 0.2/W), are currently dominating the market [10]. However, opaque PV modules often face criticism on black colored appearance, which is suited to maximize light absorption but hard to harmonize with various-colored building walls and roofs. Thus, it will be more desirable from an aesthetic viewpoint, if PV modules appear in various colors.

To fulfill the demand of colored PV modules, inorganic Bragg reflectors incorporated PV modules have been suggested [11–15]. In

* Corresponding author.

** Corresponding author.

*** Corresponding author.

E-mail addresses: ghkang@kier.re.kr (G. Kang), wkbae@skku.edu (W.K. Bae), hj.song@seoultech.ac.kr (H.-J. Song).

¹ B.G.J, D.H. contributed equally.

general, Bragg reflectors consist of multiple stacks of two different inorganic dielectric layers, whose thicknesses and refractive indices determine apparent colors perceived by human eyes. Vacuum based high temperature process is widely adopted to precisely control the thickness of dielectric layers in the reflectors, but these methods require complicated manufacturing processes along with massive, expensive infrastructures. Furthermore, a limited range of viewing angles hides the advantages of the reflectors. Broadening their reflection band, which is a common strategy to maintain their perceived colors in all directions, results in additional photon losses in the colored module with reflector [4,13,16,17].

An alternative approach to award aesthetical merits to the PV module is implanting a luminescent down-shift (LDS) color layer on the top of cells. The LDS layer contains luminophores that convert high energy ultraviolet (UV) photons to lower energy visible light. A distinct advantage of colored PV modules with LDS layers, compared to the ones with reflectors, is angle invariance of apparent colors that arise from randomly re-emitted light by luminophores. Additionally, the LDS layer would provide various colors to PV modules with diminished optical losses by exploiting high energy photons that are not efficiently used in PV modules [18–21].

Among the candidates for luminophores (organic dyes [21,22], phosphors [23] and colloidal quantum dots (QDs)), organic dyes have been widely accepted for the colored PV module, due to their high photoluminescence quantum yield (PL QY). However, their absorption spectra are typically positioned in the visible region, and they do not

efficiently convert UV to low energy light. Considering the high solar photon flux and the external quantum efficiency (EQE) of photovoltaic modules at visible light (450–700 nm), large amounts of solar photons would be consumed by the organic luminophore instead of harvested by PVs. Additionally, a limited extent of Stokes shift of organic luminophores (typically less than 50 nm) [18,22,24] stimulates self-absorption processes in condensed films, which lead to the reduction of the down-converting efficiency. Consequently, the attainable power of colored PV modules with organic luminophores is limited.

As an alternative, QDs have attracted particular interest due to their excellent PL QY close to the unity, facile color tunability over the entire visible range, high extinction coefficient at UV region, and cost-effectiveness based on solution processing [25]. Despite promises of QD luminophores, their practicable use is lagging behind owing to the materials toxicity of QDs (i.e., CdSe/CdS [26,27], CdTe [27], CdSe/CdZnS [28], and Mn²⁺ doped ZnCdS/ZnS [29]). QDs made of alternative compounds, for instance, Si [30], ZnSe/ZnS [31], CuInS₂/ZnS [32,33], and CuGaS₂/ZnS [34], have been suggested, but their spectral bandwidths (FWHM > 60 nm) are far inferior to conventional organic dyes [18,22,24] and their appearances are almost colorless because of the low contents of QDs (<1.5 mg/mL or 1 wt%) in LDS layer.

Here, we present efficient, colorful PV modules by employing InP/ZnSe_xS_{1-x} core/shell QDs. Specifically, we design the structure and composition of core/thick-shell QDs to fulfill various colors with high PL QYs and substantially enhanced absorption nearby the UV region. A

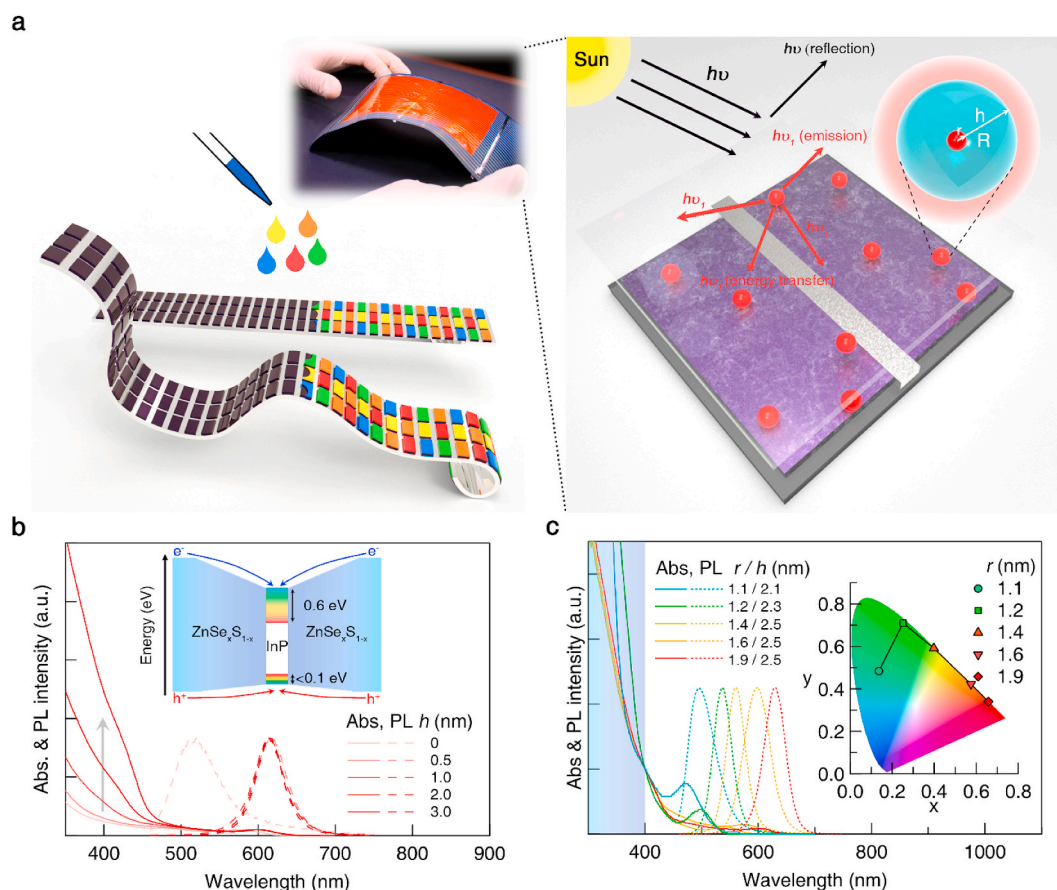


Fig. 1. Schematic illustrations of colored PV modules with QD-LDS layers and optical characteristics of InP/ZnSe_xS_{1-x} QD luminophores with varying core and shell dimensions. (a) Schematic illustrations and photograph of colored photovoltaic modules with QD LDS layers and their operation mechanism with InP/ZnSe_xS_{1-x}/ZnS QDs (inset: structure of InP/ZnSe_xS_{1-x} QDs, r: core radius, h: shell thickness, R: total radius), (b) absorption (normalized at 1S excitonic peak) and PL spectra of InP/ZnSe QDs (r = 1.2/h_{ZnSe} = 0–3.0 nm) in solution (inset: electronic structure of InP/ZnSe_xS_{1-x} QDs), (c) absorption (normalized at 450 nm) and PL spectra of InP/ZnSe_xS_{1-x} QDs with various core radius (r: core radius, h: ZnSe_xS_{1-x} shell thickness). The inset shows the calculated color coordinates from the PL spectra of InP/ZnSe_xS_{1-x} QDs in CIE 1931 chromaticity diagram.

comparative study using industrial standard opaque PV modules reveals that InP/ZnSe_xS_{1-x} QD LDS layer provides various colored appearances with high contents of QD (from cyan to deep red) to blacked PV module with minimized sacrifice of incident photon (less than 10%). Additionally, the modification of ligand for QDs paves the way for realizing the stable operation of colored PV modules under high temperature and humidity conditions.

2. Results and discussion

Fig. 1a illustrates the proof of concept devices that employ QD luminophore films on the front cover glass of commercialized rigid c-Si (p-type monocrystalline, PERC structure, and PCE of ~19% from Shin-sung E&G) and flexible stainless-steel based CIGS PV modules (cell PCE of ~12% from Hanergy). The module consists of QD-LDS coated glass/poly (ethylene-vinyl acetate) (EVA) encapsulation layer/PV cell/EVA/back sheet. In such a device architecture, the incident solar photons follow one of three pathways: (i) reflected at the surface of the front

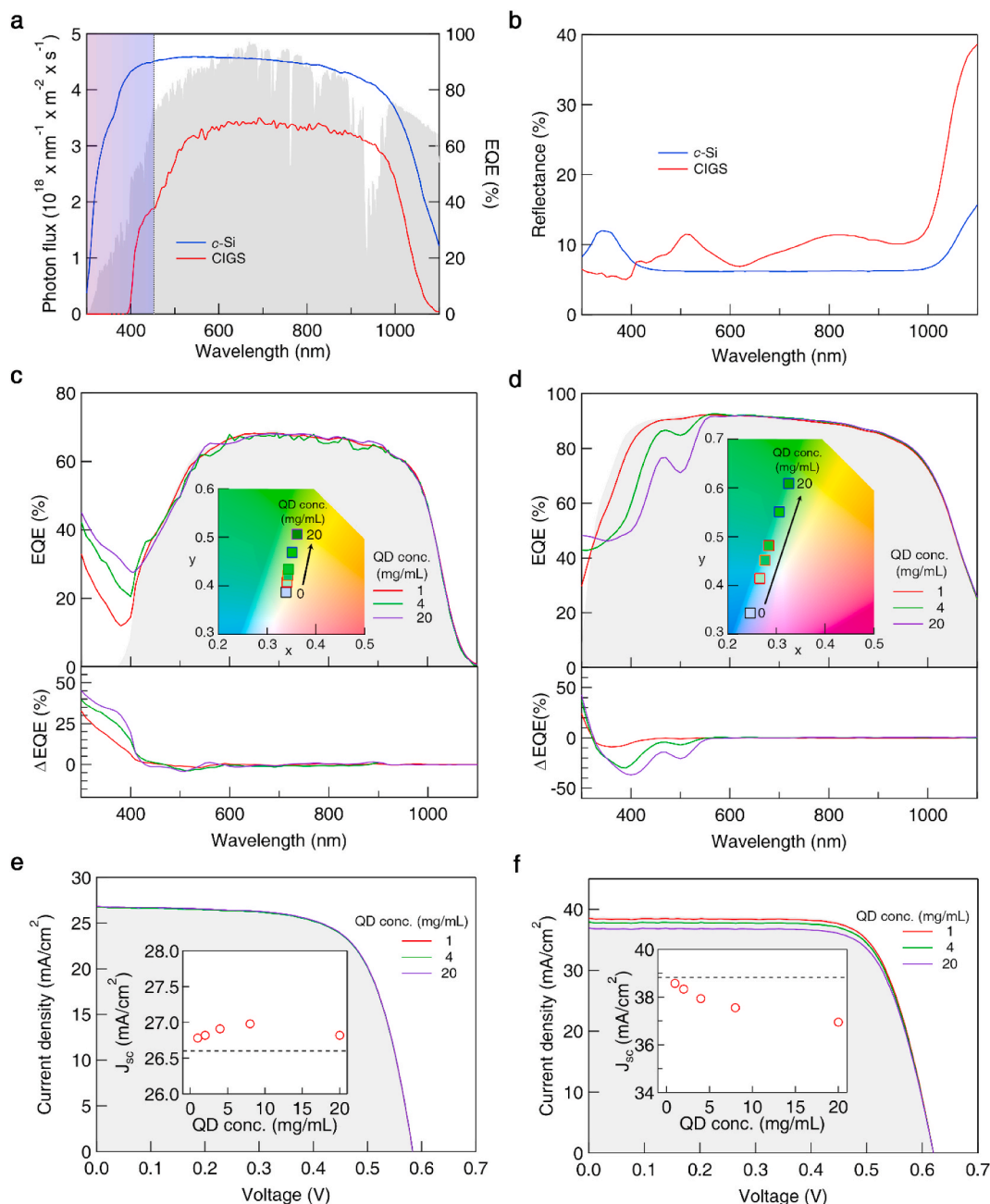


Fig. 2. The impact of QD-LDS layers with varying QD contents on optoelectronic performances and aesthetic features of flexible CIGS and c-Si PV modules.

(a) Spectral photon flux under AM 1.5G condition with EQE spectra of flexible CIGS (red) and c-Si PV (blue) modules. The filled area (grey) in (a) represents the spectral photon flux. (b) Reflectance spectra of flexible CIGS (red) and c-Si (blue) PV modules. EQE spectra of (c) flexible CIGS and (d) c-Si PV modules with varying concentrations of green InP ($r = 1.2$ nm)/ZnSe_xS_{1-x} ($h = 2.3$ nm) QD solutions (i.e., 1, 4, 20 mg/mL are represented with red, green, and purple lines, respectively). For a clear comparison, the change of EQE (Δ EQE) spectra are included. The inset graphs are the color coordinates of the corresponding PV modules on the CIE 1931 chromaticity diagram and the dotted line indicates the J_{sc} value of reference PV modules. Current density – Voltage (J–V) curves of (e) CIGS and (f) c-Si PV modules with various concentrated QDs in solution (1 (red), 4 (green), 20 (purple) mg/mL). For comparison of loss by LDS layer, J_{sc} versus QD concentration graphs are included in each case. The filled area (grey) in (c–f) and the guideline of J_{sc} value in inset of Fig. 2(e–f) represent the reference data of the PV module without QDs.

glass and each interface between layers due to the refractive index difference, (ii) absorbed and re-emitted by QD luminophores, (iii) penetrating the front layer, absorbed by active layer in the solar cell and converted into electricity. The combination of (i) reflected and (ii) re-emitted photons from QD luminophores determines the color of PV modules. Thus, the color of PV modules can be tailored upon the optical bandgap (emissive color) of core/shell QDs, mainly determined by the InP core dimension. Considering the near unity (>90%) EQE of recently developed highly efficient PVs at the visible region, the efficiency of colored PV modules is dictated by the down-conversion efficiency of photons at UV region into ones at the visible region by QD luminophores. Therefore, the sophisticated design of QD heterostructure plays an important role in achieving high-performance, colored PV modules.

We adopt toxic element (Cd or Pb) free QDs made of InP cores passivated by $\text{ZnSe}_x\text{S}_{1-x}$ composition gradient shell layers, wherein the size of the InP core defines the color, while the volume of $\text{ZnSe}_x\text{S}_{1-x}$ shells contributes to the extinction coefficient at UV region (Fig. 1b). InP cores with varying radius (r) of 1.1, 1.2, 1.4, 1.6 and 1.9 nm are prepared to express cyan, green, yellow, orange, and red colors, respectively. The thicknesses (h) and composition profiles of $\text{ZnSe}_x\text{S}_{1-x}$ shell layers are delicately engineered for each core to maximize absorption at the UV region and PL QYs. In principle, S rich $\text{ZnSe}_x\text{S}_{1-x}$ (or ZnS) outermost shell is adopted to confine photo-excited charge carriers within the core, and Se rich $\text{ZnSe}_x\text{S}_{1-x}$ (or ZnSe) inner shell is employed to mitigate the compressive lattice strain between InP core and the ZnS exterior shell (~7.7%). For smaller InP core whose lowest quantized electronic energy level resides at a higher position, larger S contents $\text{ZnSe}_x\text{S}_{1-x}$ inner shell layer is required to effectively confine the charge carriers (particularly electrons) for achieving high PL QYs [35]. Simultaneously, the maximum Se content in $\text{ZnSe}_x\text{S}_{1-x}$ shell is intended for a thick shell to absorb more UV light as well as the small overlap between absorption and PL spectra, while keeping high PL QYs. The significantly enhanced absorption at the UV region by the $\text{ZnSe}_x\text{S}_{1-x}$ shell is well presented in Fig. 1b. In this study, we use InP ($r = 1.2$ nm)/ $\text{ZnSe}_{0.33}\text{S}_{0.67}$ (1.0 nm)/ZnS (1.3 nm) for green ($\lambda_{\text{peak}} = 535$ nm, FWHM = 38 nm, PL QY = 85%) and InP ($r = 1.9$ nm)/ ZnSe (2.0 nm)/ZnS(0.5 nm) QDs for red ($\lambda_{\text{peak}} = 630$ nm, FWHM = 40 nm, PL QY = 85%), respectively. The optimal structures and optical properties of QDs are detailed in Supplementary data.

Fig. 2a–b demonstrate optoelectronic and optical responses upon the wavelength of incident photons of rigid c-Si and flexible CIGS PV modules. The discrepancy observed in the EQE curves of rigid c-Si versus flexible CIGS PV modules is mainly attributed to the surface photonic structures and the optical materials adopted in PVs. With the assistance of the pyramid-shaped anti-reflective structure, the industry standard c-Si PV exhibits EQE over 80% at entire visible and NIR regions (400–1000 nm). By contrast, the thin CIGS module that is assembled with UV-absorbing flexible polymer and CdS buffer layer show decreased spectral response, particularly in the UV and deep blue region. Regardless of PV types, both modules exhibit a sharp EQE drop at UV region (less than 400 nm) whereby the photon absorbance by QD luminophores is substantial due to the thick $\text{ZnSe}_x\text{S}_{1-x}$ shells. These features promise that colored PV modules with better efficiency or at

least marginal efficiency loss can be attained by inserting the QD-LDS layer.

To investigate the influence of optical properties of QD films, we measure the performances of PV modules with QD dispersions in toluene with various concentrations (1–20 mg/mL) into a quartz cell in a wide range of wavelength (300–1100 nm). Fig. 2c–f represent the impact of green-emitting QD ($r = 1.2$ nm/ $h = 2.3$ nm)-LDS layers on the performance of CIGS and c-Si PV modules. Here, quartz cuvettes ($40 \times 10 \times 1$ mm³) containing QD dispersion with various concentrations are placed on the front of PV modules with index matching oil. Flexible CIGS PV modules exhibit a notable increase in EQE at the UV and deep blue region (at most over 40%), which comes from the LDS effect of the QD layer by converting unused high energy photons to the green band ($\lambda_{\text{peak}} = 535$ nm). The inevitable absorption of QD during the LDS process marginally decreases EQEs at blue to green region (less than 5%). Nevertheless, the photon gain at the UV region surpasses the photon loss at the visible region by the QD-LDS layer, leading to the increase in both the short circuit current (J_{sc}) and power conversion efficiency (PCE) of green-colored CIGS PV modules regardless of the QD contents (Fig. 2e and Table 1). Thus, our QD-LDS layer does not only provide a colorful outlook of CIGS PV modules but also improves the spectral response of devices by utilizing high energy photons in deep blue and UV regions.

Similar trends, EQE gain at UV region and EQE loss at the visible region, but at different extents are observed in the case with the c-Si PV modules (Fig. 2d). The narrow window for photon gains but greater efficiency loss at a wider range in the visible band by the QD-LDS layer yields the reduction of J_{sc} and PCEs of c-Si PV modules (Fig. 2f). The extent of efficiency loss becomes greater for the LDS layer with greater QD contents. Since recently developed efficient PV cells (CIGS, GaAs, CdTe, and perovskite) also effectively collect high energy photons (UV light) [36], similar sacrifice for the color appearance of modules is expected. Despite losses in visible light, it is noteworthy that a green-colored c-Si PV module with CIE index of (0.33, 0.51) can be obtained at a cost of the marginal PCE drop (17.23%→16.37%).

Theoretically, the EQE of the PV module with a LDS layer at a specific wavelength (λ) ($\text{EQE}_{\text{LDS}}(\lambda)$) is defined as below:

$$\text{EQE}_{\text{LDS}}(\lambda) = (1 - \eta_{\text{abs}}(\lambda))\text{EQE}(\lambda) + \eta_{\text{abs}}(\lambda)\eta_{\text{PL QY}}\eta_{\text{opt}}\text{EQE}_{\text{Avg}} \quad (1)$$

where EQE (λ) is the EQE of a module without LDS layer at a specific wavelength (λ), η_{abs} is absorptance of a LDS layer, $\eta_{\text{PL QY}}$ is PL QY of luminophores, η_{opt} is the optical efficiency of re-emitted photons to reach the cell, and EQE_{Avg} is average internal quantum efficiency of PV module at the emission spectrum of luminophore. Detailed procedure to derive ideal η_{opt} is elucidated in supplementary data, while the others are empirically obtained. Given $\eta_{\text{PL QY}}$ of QDs (85%), η_{opt} of infinite large LDS film (87.5%), and EQE_{Avg} of CIGS module (75%), the attainable maximum EQE of colored CIGS PV module is 55% ($= 0.85 \times 0.875 \times 0.75 \times 0.98$) at 300 nm, where most of the photons are absorbed by QD-LDS ($\eta_{\text{abs}} = 0.98$) [37–39]. Moreover, theoretically expected EQE of c-Si PV module with the LDS layer is 66% ($= 0.85 \times 0.875 \times 0.9 \times 0.98$) at 300 nm. However, the measured EQEs of CIGS (45%) and c-Si (48%) PV

Table 1

Device characteristics of CIGS and c-Si PV modules employing InP ($r = 1.2$ nm)/ $\text{ZnSe}_x\text{S}_{1-x}$ ($h = 2.3$ nm) green-emitting QDs with varying contents.

QD contents (mg/mL)		0	1	2	4	8	20
CIGS ^a	EQE @ 300 nm (%)	0	33.0	40.7	42.1	45.1	45.3
	J_{sc} (mA cm ⁻²)	26.60	26.78	26.82	26.91	26.98	26.82
	ΔJ_{sc} (%)	–	+0.7	+0.8	+1.1	+1.4	+0.8
	PCE (%)	10.69	10.77	10.78	10.81	10.84	10.78
	CIE color index (x, y)	(0.39, 0.34)	(0.41, 0.34)	(0.34, 0.42)	(0.34, 0.43)	(0.35, 0.47)	(0.36, 0.51)
c-Si	EQE @ 300 nm (%)	5.7	29.7	36.7	43.0	47.5	48.3
	J_{sc} (mA cm ⁻²)	38.82	38.57	38.33	37.94	37.55	36.95
	ΔJ_{sc} (%)	–	- 0.6	- 0.6	- 1.0	- 1.0	- 1.6
	PCE (%)	17.23	17.12	17.00	16.82	16.65	16.37
	CIE color index (x, y)	(0.25, 0.24)	(0.27, 0.31)	(0.28, 0.35)	(0.28, 0.38)	(0.31, 0.45)	(0.33, 0.51)

^a All measurement was conducted without any light soaking.

modules are lower than their corresponding simulated values. We believe that the reabsorption, scattering, and waveguide mode in the LDS layer, those are not regarded in the ideal case simulation, provoke additional efficiency loss in the real device [25,40]. If further studies of ideal luminophores (unity PL QY with zero-reabsorption) and optical structure are successfully conducted, loss-free colored PV modules will be realized even in highly efficient cells, as explained in Supplementary data.

Controlling the dimension of InP/ZnSe_xS_{1-x} QDs awards a variety of colors to c-Si PV modules (Fig. 3, Table 2). To systematically analyze the

device performance of colored modules with high contents of QDs, five different InP/ZnSe_xS_{1-x} QD films incorporated c-Si PV modules are fabricated. The overall device structure is QD LDS-coated glass/EVA/solar cell/EVA/black back sheet. To generate colors by converting UV and deep blue light, QD-LDS film is casted in front of EVA layer, which absorb UV light to protect cell. The spectra of full-colored c-Si PV modules with different LDS layers measured under AM 1.5 G condition are displayed in Fig. 3a. Along with the reflected lights from the front glass and PV cell (Fig. 2b), the PL emanating from QD-LDS films present aesthetic appeals to black rigid PV modules. The use of cyan, green,

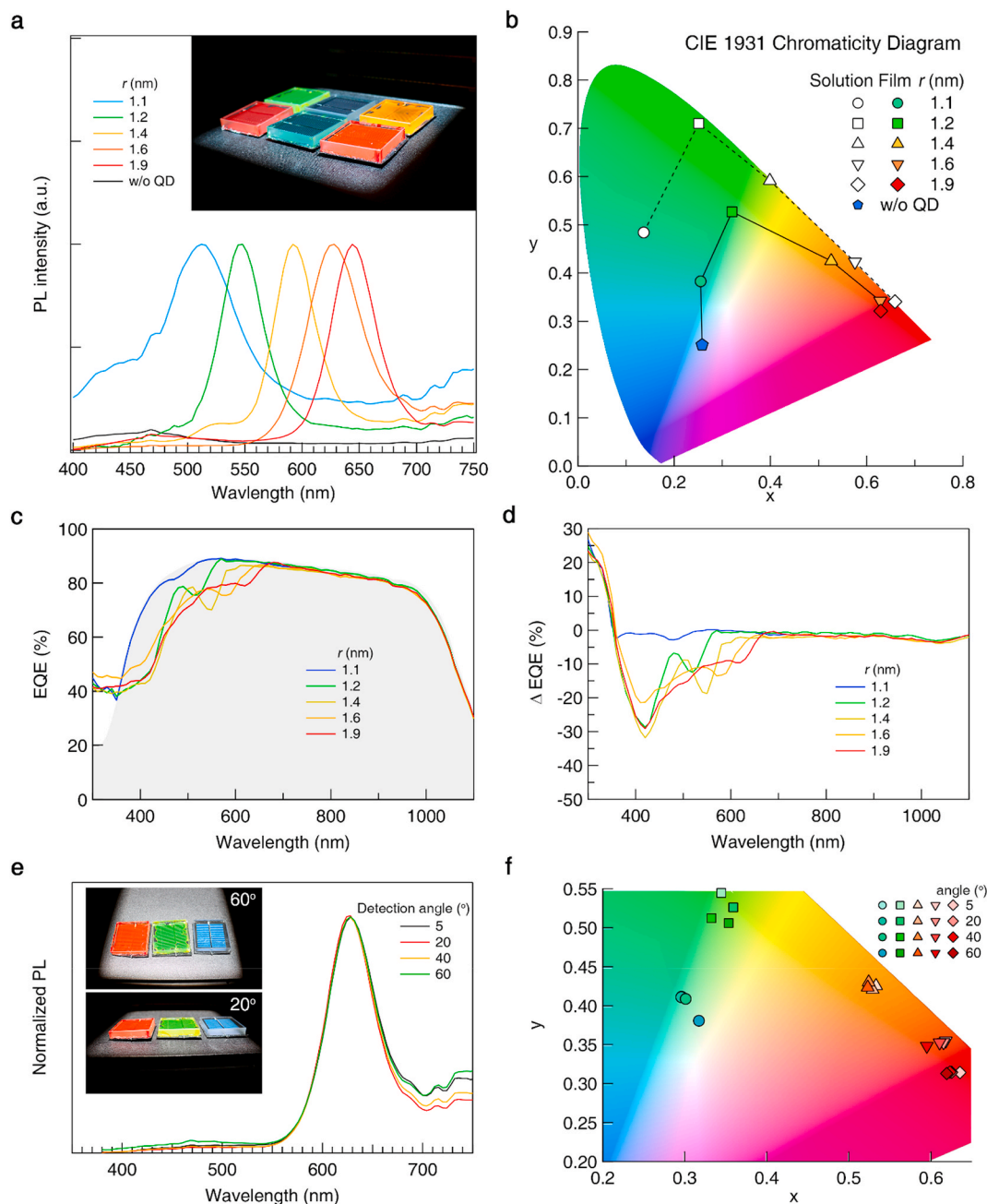


Fig. 3. The impact of QD-LDS films with varying colors on optoelectronic performances and aesthetic features of rigid c-Si PV modules. (a) Normalized emission spectra, (b) color coordinates (CIE 1931 chromaticity diagram), (c) EQE, and (d) Δ EQE of the colored c-Si PV modules employing QD-LDS film (coated in a front glass) with various core radius ($r = 1.1$ (circle), 1.2 (square), 1.4 (triangle), 1.6 (inverse triangle) and 1.9 nm (diamond)) under AM 1.5G illumination. The inset of (a) is a photograph of actual c-Si PV modules with QD-LDS film. The measured color coordinates of the colored c-Si PV module with QD film (filled) and calculated result from the PL spectrum of QDs in solution (open) are marked on the CIE 1931 chromaticity diagram in the (b). The filled area (grey) represents the EQE spectrum of reference module without the QD-LDS layer. (e) The normalized emission intensity of the colored PV modules ($r = 1.6$ nm) measured at different viewing angles. The inset is photographs of the colored PV modules taken at 20° and 60°. (f) The color coordinates of each colored c-Si PV module monitored at different viewing angles. In all cases, their color coordinates are varied within the small range (Δx and $\Delta y \leq 0.05$).

Table 2Device characteristics of c-Si PV modules employing InP/ZnSe_xS_{1-x} QD-LDS layers with various core radius.

InP/ZnSe _x S _{1-x} QDs (r/h, nm)	EQE (% , @ 300 nm)	CIE color index (x, y)	V _{oc} (V)	J _{sc} (mA cm ⁻²)	FF	PCE (%)
w/o QDs	18.2	(0.26, 0.25)	0.65	38.1	73.4	17.5
1.2/2.1	44.9	(0.25, 0.38)	0.64	37.6	73.3	17.2
1.2/2.3	42.9	(0.32, 0.53)	0.64	36.5	72.8	16.6
1.4/2.5	41.3	(0.53, 0.43)	0.65	34.9	72.6	16.4
1.6/2.5	47.1	(0.63, 0.34)	0.65	34.8	73.0	16.2
1.9/2.5	41.6	(0.63, 0.32)	0.64	34.9	71.4	15.8

yellow, orange, and red-emitting QDs, whose PL spectra reside on the periphery of the CIE coordinate, aid us in achieving a wide range of colors in PV modules (Fig. 3b). Aforementioned in the case with green QDs, the introduction of QD luminophores accompanies the inevitable sacrifice of incident photons at the visible region (Fig. 3c and d). The smaller the optical bandgap of InP core becomes, the broader range of spectra the device efficiency forfeits. Benefitted from the thick shell geometry of InP/ZnSe_xS_{1-x} QDs that enables to minimize the efficiency loss by recycling barely used UV light, the efficiency loss as a trade-off of aesthetic appeals is less than 10% even in red-colored PV modules (9.7%) (Table 2). As a result of absorption of visible light by QD layer, the loss of photons is inevitable in yellow, orange, and red colored modules. If further modification of QD is conducted to maximize its stoke shift and PL QY, the loss will be decreased, as marked in supplementary data. It should be noted that the efficiency loss in non-optimized our system is less than or at least comparable to that with Bragg reflector based commercially available colored modules [11,15]. Despite excellent performance of our suggested color PV module in the point of color and efficiency, it is very hard to demonstrate vivid blue color module in our approach. Since luminophores present color throughout down-converting process, their inherent limitation is to generate high energy light, such as deep blue. We believe that the further studies, e. g. introduction of blue colored PV cells to our structure, will enable one to utilize full colored PV modules.

The beauty of QD-LDS incorporated PV modules, compared to the case with Bragg reflectors, is the angular invariance of apparent colors. Independent to the angle, the peak of the color spectrum from the colored PV module with the QD-LDS layer is fixed. Moreover, only small change of color coordinator (Δx and $\Delta y \leq 0.05$) was observed, when the viewing angle varies from 0 to 60° (Please see Fig. 3e and f). In Bragg reflectors, a stack of more than two materials having different refractive indices form alternating multilayered structures with a certain periodicity, which creates a photonic bandgap that corresponds to the wavelength of reflected lights. However, the peak of the reflection band of the Bragg reflector is normally shifted to oblique incident light because of the elongated light path. Thus, strong angular dependence and color distortion are challenge issues in Bragg reflector-based color PV module. By contrast, PL emission by QDs maintains its color regardless of incident or view angle. Consequently, the angular insensitive QD incorporated colored PV module is more acceptable to BIPV systems, which are normally installed various positions and direction of the building.

Stable operation of colored PV modules at outdoor conditions require structural robustness of QD-LDS layers against exposure to heat and moisture. QDs retain a large proportion of surface atoms (>10% of entire atoms) that are subject to undergo photochemical degradation via surface oxide, and hence the stabilization of the QD surface is vital to secure their photophysical properties. The surface oxidation process involves the dissociation of ligands by leaving unpassivated surface atoms [41,42] that are liable to undergo the chemical reaction with reactive chemical species (e.g., oxygens). Ligands with strong binding affinity to Zn atoms are expected to suppress the surface reaction, enabling long-term stable operation of colored PV modules [43–45]. As synthesized QDs are passivated with the carboxylate ligands (e.g., oleic acids (OAs)) that are used to stabilize the cations (In³⁺ and Zn²⁺) during QD growth. We displace the native oleate ligands to the ones with thiol binding groups that hold stronger binding affinity to the surface Zn

atoms (46.5 kcal/mol for Zn-S_{thiol} versus 11.9 kcal/mol for Zn-carboxylate) [46,47]. To maximize the binding affinity, we also test the bidentate ligands comprising the combinations of carboxylate (-COO⁻) and thiolate (-S⁻) binding groups (Fig. 4a). The ligand

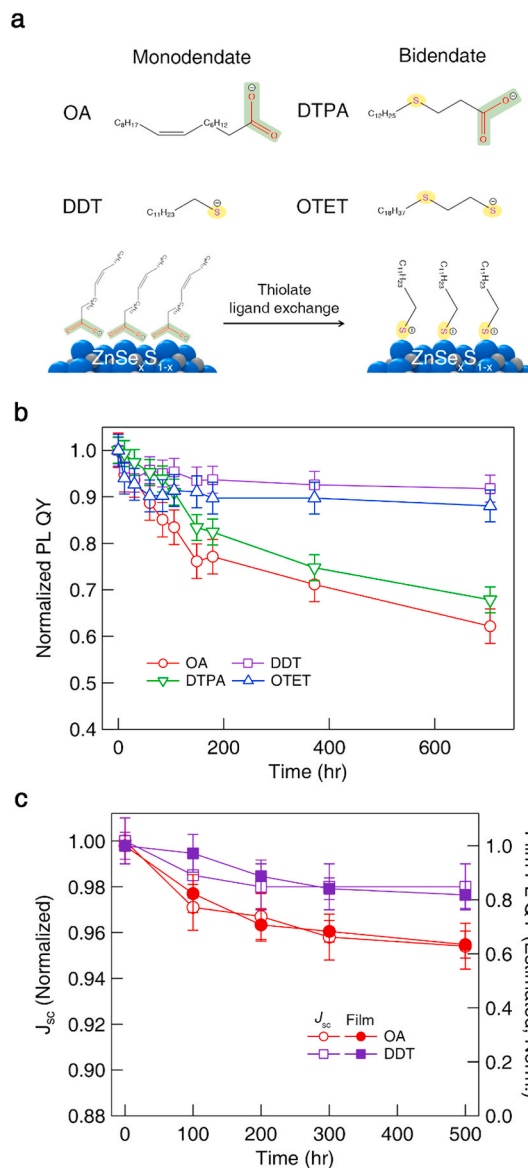


Fig. 4. Thermal stability of InP/ZnSe_xS_{1-x} QDs before and after ligand modification. (a) The molecule structures of ligands used in this study (Oleate [OA], 1-dodecanethiolate [DDT], 3-(dodecylthio) propanoate [DTPA] and 2-(octadecylthio) ethane thiolate [OTET]) and schematic illustration of the ligand displacement from native OA to DDT ligands, (b) normalized PL-QY of QD (solution) capped with various ligands as a function of exposure time under ambient room light, (c) normalized J_{sc} of red-colored c-Si PV module and estimated PL QY of InP (r = 1.9 nm)/ZnSe_xS_{1-x} (h = 2.5 nm) QD-LDS films capped with different ligands (OA and DDT) as a function of damp heat test time (85 °C/85% RH).

displacement from oleate ligands to the thiolate ones take spontaneously in solution at room temperature (Supplementary data). We note that the ligand displacement does not accompany any notable change in the photophysical properties of QDs.

Prior to the device test, we examine the impact of the types of ligands on the photochemical stability of QDs (Fig. 4b). The stability of QDs, capped with various ligands (*i.e.*, carboxylate *versus* thiolate, or monodentate *versus* bidentate), is monitored through their PL QY change at the ambient condition with a room light. The PL QY of QDs passivated with thiol ligands (1-dodecanethiol or 2-(octadecylthio)ethanethiol) is degraded less than 10% after 720 h of exposure to air. In contrast, QDs passivated with oleate ligands show 30% of PL QY drop. Interestingly, in the chosen variation of ligand structure, notable enhancement with respect to the photostability of QDs is not observed for the bidentate ligands compared to the monodentate ones. This implies that the packing density of ligands on QD surface and their bonding strength [43,48] should be taken into account when designing the passivation ligands [49].

QDs stabilized with mono-thiolate ligands preserve their photophysical properties in film, and their down-conversion characteristics in modules during damp heat test (DH, 85 °C and 85% relative humidity) (Fig. 4c). Specifically, the colored PV module having thiol capped QDs shows slow decay behavior than that of the module with carboxylate capped ones after 500 h of DH. Simultaneously, the LDS film with oleate capped QDs undergoes 30% of PL QY loss after 500 h of DH, while the one with thiolate ligands tolerate heat and humidity as proven minor degradation of PL QY (<15%) (Fig. 4c). The comprehensive result based on the module and spectroscopic analysis undoubtedly implies that the surface-modified QD layers would allow them to be used as an element for outdoor operating, energy harvesting systems.

The structural engineering of QD luminophores enables to minimize the sacrifice of photons and more reliable performance of colored PV module. The design of thick $\text{ZnSe}_x\text{S}_{1-x}$ shell in QDs captures more photons, achieves high PL QY, and yields a small overlap between absorption and emission spectra. Furthermore, the surface stabilization with short ligands upholds their optical properties against the heat and humidity. Since the optical properties of quantum dots are still inferior to the state-of-the-art organic dye molecules, we believe that further improvements from achieving near-unity PL QYs in eco-friendly QDs and suppression of energy transfer within the QD film will boost the higher efficiency and more saturated colors in the QD-LDS, even in the case of green and cyan colors. Advances in the fundamental material design combined with ideal optical structure with reduced scattering will lead to the realization of an efficiency-loss free, stable colored PV module.

3. Conclusions

In summary, we demonstrate various colored PV modules with luminescent down-shift layers employing eco-friendly $\text{InP}/\text{ZnSe}_x\text{S}_{1-x}$ QD luminophores. The thick $\text{ZnSe}_x\text{S}_{1-x}$ shell is grown not only to confine photo-excited charge carriers into the emissive InP core and but also to boost absorption of high energy photons. Moreover, by controlling the size of the core, vivid full color appealing InP QDs (495–625 nm) are achieved with over 80% of PL QYs. With the assistance of structurally engineered QDs, the colored PV modules exhibit over 40% EQE improvement at UV region and less than 15% of incident photons sacrifice for full color decoration. Moreover, the color emanating from QD incorporated PV modules is angular invariant and its color gamut is wide to express various colors. Furthermore, the reliability of colored PV module can be enhanced by introducing stable, thiol capped QDs. Therefore, the introduction of $\text{InP}/\text{ZnSe}_x\text{S}_{1-x}$ QDs to the PV module will contribute to the versatile deployment of an aesthetic PV system.

4. Experimental section

Fabrication of colored opaque PV modules with $\text{InP}/\text{ZnSe}_x\text{S}_{1-x}$ QDs: In order to demonstrate colored PV module in Fig. 3, $\text{InP}/\text{ZnSe}_x\text{S}_{1-x}$

QD film ($50 \times 50 \text{ mm}^2$) was casted on the cleaned quartz glass through spin-coating (1000 rpm, 30 s) of its solution ($\sim 150 \text{ mg/mL}$ with toluene). However, slot die, ink jet printing, and spray coating, which are widely accepted for large sized substrate, would allow us to fabricate large sized QD coated glass or front film, as displayed in the inset of Fig. 1a. After that, ribbon connected c-Si solar cell, sandwiched by 0.3 mm thick ethylene vinyl acetate (EVA) films, was assembled with QD coated glass and black back sheet. And then, the assembly of QD coated glass/EVA/solar cell/EVA/black back sheet was laminated under vacuum ($\sim 0.1 \text{ Torr}$) and high temperature ($\sim 150 \text{ }^\circ\text{C}$) for 20 minutes. Finally, the module was cooled at room temperature for 30 minutes.

Device Characterization: We characterized the PV modules with QD in solution (Fig. 2) and QD-LDS film (Fig. 3). The performance of colored PV module was characterized under xenon lamp with AM 1.5 G filter (Xe 1000, McScience) and 100 mW/cm^2 radiant power. The color coordinator of them was monitored by a spectroradiometer (CS 2000, Konica Minolta) under AM 1.5 G condition. In the chromaticity measurement, baffles were applied to remove noise signal from the direct reflection of the incident light. The estimated film PL QY of QD-LDS layer in colored PV modules were calculated from the ratio between the PL decay lifetime obtained from the film ($\tau_{1/e}$) and the radiative exciton recombination rate (τ_r) [50,51].

$$PL\ QY_{film} = PL\ QY_{solution} \times \tau_{1/e} / \tau_r \quad (2)$$

Characterization of PV modules with QD in solution: Meanwhile, the effect of QD density on the external quantum efficiency of various PV modules was analyzed using QD solution loaded quartz cuvettes ($10 \times 40 \times 1 \text{ mm}^3$) (Fig. 2). To avoid optical loss between QD solution loaded cuvettes and PV module, index matching liquid (NOA 88, Norland optics), whose refractive index was 1.52 and transparent at visible as well as near UV region, was inserted between them. Then, the external quantum efficiency of them was investigated with monochromator incorporated lock-in amplifier (QEXL 10, PV measurement). The J_{SC} and PCE was calculated based on the experimentally achieved EQE of both type modules and current density-voltage (J-V) curve of ones without LDS color layer.

Stability test: The stability test of QD in solution was conducted by comparing the PL-QY change of QDs as a function of time under ambient condition and room light. The absorbance of QD in solution was fixed to 0.1 at the 1S excitonic peak of absorption spectra. The QDs in solution were stirred at 100 rpm. The QD solutions were not dry up because the solvent (toluene) was regularly added. The stability test of colored c-Si PV modules with QDs were evaluated by comparing their performances. Moreover, the PL decay dynamics of QD LDS film was checked as a function of time. The test was proceeded in a closed chamber under 85 °C/85% relative humidity conditions for 200 h. The fabricated device was inserted after the chamber stabilized at constant temperature and humidity. During the stability test, the performances of device and PL decay dynamics of QD LDS layers in device were monitored under ambient conditions.

CRedit authorship contribution statement

Byeong Guk Jeong: Writing - original draft, Formal analysis, Investigation. **Donghyo Hahm:** Writing - original draft, Formal analysis. **Jeong Woo Park:** Formal analysis, Validation. **Jun Young Kim:** Formal analysis, Investigation. **Hee-Eun Song:** Writing - review & editing. **Min Gu Kang:** Writing - review & editing. **Sohee Jeong:** Writing - review & editing. **Gihwan Kang:** Writing - review & editing. **Wan Ki Bae:** Writing - review & editing. **Hyung-Jun Song:** Conceptualization, Simulation, Supervision, Writing - review & editing.

Declaration of competing interest

The authors declare that they have no known competing financial

interests or personal relationships that could have appeared to influence the work reported in this paper.

Acknowledgements

This work is supported by Nanomaterials Technology Development Program (2019M3A7B4063239), Creative Materials Discovery Program (NRF-2019M3D1A1078299) and the Basic Science Research Program (NRF-2019R1F1A1057693) through the National Research Foundation of Korea and grant funded by the Ministry of Education (2020R1I1A1A01069324) and by the Ministry of Science and ICT (2020M3D1A2101319, 2020R1A2C2011478, NRF-2020M3H4A1A01086888). H.-E. S., M. G. K., G. H. K., and H.-J. S. acknowledge the New & Renewable Energy Technology Development Program of the Korea Institute of Energy Technology Evaluation and Planning (KETEP) grant, funded by the Ministry of Trade, Industry and Energy, Korea (No. 20193010014570).

Appendix A. Supplementary data

Supplementary data to this article can be found online at <https://doi.org/10.1016/j.nanoen.2020.105169>.

References

- [1] J. Trube, M. Fischer, G. Erfurt, C.-C. Li, P. Ni, M. Woodhouse, A. Metz, I. Saha, J. Bai, Q. Wang, VDMA, Deutschland, 2019.
- [2] N.M. Haegel, H. Atwater, T. Barnes, C. Breyer, A. Burrell, Y.-M. Chiang, S. De Wolf, B. Dimmler, D. Feldman, S. Glunz, J.C. Goldschmidt, D. Hochschild, R. Inzunza, I. Kaizuka, B. Kroposki, S. Kurtz, S. Leu, R. Margolis, K. Matsubara, A. Metz, W. K. Metzger, M. Morjaria, S. Niki, S. Nowak, I.M. Peters, S. Philipps, T. Reindl, A. Richter, D. Rose, K. Sakurai, R. Schlattmann, M. Shikano, W. Sinke, R. Sinton, B. J. Stanbery, M. Topic, W. Tumas, Y. Ueda, J. van de Lagemaat, P. Verlinden, M. Vetter, E. Warren, M. Werner, M. Yamaguchi, A.W. Bett, Terawatt-scale photovoltaics: transform global energy, *Science* 364 (2019) 836–838, <https://doi.org/10.1126/science.aaw1845>.
- [3] K. Lee, N. Kim, K. Kim, H.-D. Um, W. Jin, D. Choi, J. Park, K.J. Park, S. Lee, K. Seo, Neutral-colored transparent crystalline silicon photovoltaics, *Joule* 4 (2020) 235–246, <https://doi.org/10.1016/j.joule.2019.11.008>.
- [4] A. Røyset, T. Kolås, B.P. Jelle, Coloured building integrated photovoltaics: influence on energy efficiency, *Energy Build.* 208 (2020) 109623, <https://doi.org/10.1016/j.enbuild.2019.109623>.
- [5] F. Meinardi, F. Bruni, S. Brovelli, Luminescent solar concentrators for building-integrated photovoltaics, *Nat. Rev. Mater.* 2 (2017) 17072, <https://doi.org/10.1038/natrevmats.2017.72>.
- [6] M.R. Bergren, N.S. Makarov, K. Ramasamy, A. Jackson, R. Guglielmetti, H. McDaniel, High-performance CuInS₂ quantum dot laminated glass luminescent solar concentrators for windows, *ACS Energy Lett.* 3 (2018) 520–525, <https://doi.org/10.1021/acsenergylett.7b01346>.
- [7] G.J. Faturrochman, M.M. de Jong, R. Santbergen, W. Folkerts, M. Zeman, A.H. M. Smets, Maximizing annual yield of bifacial photovoltaic noise barriers, *Sol. Energy* 162 (2018) 300–305, <https://doi.org/10.1016/j.solener.2018.01.001>.
- [8] S.R. Wadhawan, J.M. Pearce, Power and energy potential of mass-scale photovoltaic noise barrier deployment: a case study for the U.S., *Renew. Sustain. Energy Rev.* 80 (2017) 125–132, <https://doi.org/10.1016/j.rser.2017.05.223>.
- [9] M. Kanellis, M.M. de Jong, L. Slooff, M.G. Debije, The solar noise barrier project: 1. Effect of incident light orientation on the performance of a large-scale luminescent solar concentrator noise barrier, *Renew. Energy* 103 (2017) 647–652, <https://doi.org/10.1016/j.renene.2016.10.078>.
- [10] M.H. Alaaeddin, S.M. Sapuan, M.Y.M. Zuhri, E.S. Zainudin, F.M. Al-Oqila, Photovoltaic applications: status and manufacturing prospects, *Renew. Sustain. Energy Rev.* 102 (2019) 318–332, <https://doi.org/10.1016/j.rser.2018.12.026>.
- [11] S. Lee, G.Y. Yoo, B. Kim, M.K. Kim, C. Kim, S.Y. Park, H.C. Yoon, W. Kim, B.K. Min, Y.R. Do, RGB-colored Cu(In,Ga)(S,Se)₂ thin-film solar cells with minimal efficiency loss using narrow-bandwidth stopband nano-multilayered filters, *ACS Appl. Mater. Interfaces* 11 (2019) 9994–10003, <https://doi.org/10.1021/acsami.8b21853>.
- [12] C. Ji, Z. Zhang, T. Masuda, Y. Kudo, L.J. Guo, Vivid-colored silicon solar panels with high efficiency and non-iridescent appearance, *Nanoscale Horiz.* 4 (2019) 874–880, <https://doi.org/10.1039/C8NH00368H>.
- [13] J. Halme, P. Mäkinen, Theoretical efficiency limits of ideal coloured opaque photovoltaics, *Energy Environ. Sci.* 12 (2019) 1274–1285, <https://doi.org/10.1039/C8EE03161D>.
- [14] G.Y. Yoo, J.-s. Jeong, S. Lee, Y. Lee, H.C. Yoon, V.B. Chu, G.S. Park, Y.J. Hwang, W. Kim, B.K. Min, Y.R. Do, Multiple-color-generating Cu(In,Ga)(S,Se)₂ thin-film solar cells via dichroic film incorporation for power-generating window applications, *ACS Appl. Mater. Interfaces* 9 (2017) 14817–14826, <https://doi.org/10.1021/acsami.7b01416>.
- [15] G.Y. Yoo, R. Azmi, C. Kim, W. Kim, B.K. Min, S.-Y. Jang, Y.R. Do, Stable and colorful perovskite solar cells using a nonperiodic SiO₂/TiO₂ multi-nanolayer filter, *ACS Nano* 13 (2019) 10129–10139, <https://doi.org/10.1021/acsnano.9b03098>.
- [16] G. Peharz, A. Ulm, Quantifying the influence of colors on the performance of c-Si photovoltaic devices, *Renew. Energy* 129 (2018) 299–308, <https://doi.org/10.1016/j.renene.2018.05.068>.
- [17] N. Jollissaint, R. Hanbali, J.-C. Hadorn, A. Schüler, Colored solar façades for buildings, *Energy Procedia* 122 (2017) 175–180, <https://doi.org/10.1016/j.egypro.2017.07.340>.
- [18] D. Alonso-Álvarez, D. Ross, E. Klampaftis, K.R. McIntosh, S. Jia, P. Storiz, T. Stolz, B.S. Richards, Luminescent down-shifting experiment and modelling with multiple photovoltaic technologies, *Prog. Photovoltaics* 23 (2015) 479–497, <https://doi.org/10.1002/ppp.2462>.
- [19] J. Day, S. Senthilarasu, T.K. Mallick, Improving spectral modification for applications in solar cells: a review, *Renew. Energy* 132 (2019) 186–205, <https://doi.org/10.1016/j.renene.2018.07.101>.
- [20] B. McKenna, R.C. Evans, Towards efficient spectral converters through materials design for luminescent solar devices, *Adv. Mater.* 29 (2017) 1606491, <https://doi.org/10.1002/adma.201606491>.
- [21] E. Klampaftis, D. Ross, G. Kocher-Oberlehner, B.S. Richards, Integration of color and graphical design for photovoltaic modules using luminescent materials, *IEEE J. Photovolt.* 5 (2015) 584–590, <https://doi.org/10.1109/JPHOTOV.2015.2392934>.
- [22] A. Solodovnyk, C. Kick, A. Osvet, H.-J. Egelhaaf, E. Stern, M. Batentschuk, K. Forberich, C.J. Brabec, Optimization of solution-processed luminescent down-shifting layers for photovoltaics by customizing organic dye based thick films, *Energy Technol.* 4 (2016) 385–392, <https://doi.org/10.1002/ente.201500404>.
- [23] K. Bouras, G. Schmerber, G. Ferblantier, D. Aureau, H. Park, W.K. Kim, H. Rinnert, A. Dinia, A. Slaoui, S. Colis, Cu(InGa)Se₂ solar cell efficiency enhancement using a Yb-doped SnOx photon converting layer, *ACS Appl. Energy Mater.* 2 (2019) 5094–5102, <https://doi.org/10.1021/acsaem.9b00771>.
- [24] D. Ross, E. Klampaftis, J. Fritsche, M. Bauer, B.S. Richards, Increased short-circuit current density of production line CdTe mini-module through luminescent down-shifting, *Sol. Energy Mater. Sol. Cells* 103 (2012) 11–16, <https://doi.org/10.1016/j.solmat.2012.04.009>.
- [25] B.G. Jeong, Y.-S. Park, J.H. Chang, I. Cho, J.K. Kim, H. Kim, K. Char, J. Cho, V. I. Klimov, P. Park, D.C. Lee, W.K. Bae, Colloidal spherical quantum wells with near-unity photoluminescence quantum yield and suppressed blinking, *ACS Nano* 10 (2016) 9297–9305, <https://doi.org/10.1021/acsnano.6b03704>.
- [26] R. Lopez-Delgado, H.J. Higuera-Valenzuela, A. Zazueta-Raynaud, A. Ramos-Carrasco, J.E. Pelayo, D. Berman-Mendoza, M.E. Álvarez-Ramos, A. Ayon, Solar cell efficiency improvement employing down-shifting silicon quantum dots, *Microsyst. Technol.* 24 (2018) 495–502, <https://doi.org/10.1007/s00542-017-3405-x>.
- [27] S. Kalytchuk, S. Gupta, O. Zhovtiuk, A. Vaneski, S.V. Kershaw, H. Fu, Z. Fan, E.C. H. Kwok, C.-F. Wang, W.Y. Teoh, A.L. Rogach, Semiconductor nanocrystals as luminescent down-shifting layers to enhance the efficiency of thin-film CdTe/CdS and crystalline Si solar cells, *J. Phys. Chem. C* 118 (2014) 16393–16400, <https://doi.org/10.1021/jp410279z>.
- [28] H.-J. Jeong, Y.-C. Kim, S.K. Lee, Y. Jeong, J.-W. Song, J.-H. Yun, J.-H. Jang, Ultrawide spectral response of CIGS solar cells integrated with luminescent down-shifting quantum dots, *ACS Appl. Mater. Interfaces* 9 (2017) 25404–25411, <https://doi.org/10.1021/acsami.7b08122>.
- [29] I. Levchuk, C. Würth, F. Krause, A. Osvet, M. Batentschuk, U. Resch-Genger, C. Kolbeck, P. Herre, H.P. Steinrück, W. Peukert, C.J. Brabec, Industrially scalable and cost-effective Mn²⁺ doped ZnxCd_{1-x}S/ZnS nanocrystals with 70% photoluminescence quantum yield, as efficient down-shifting materials in photovoltaics, *Energy Environ. Sci.* 9 (2016) 1083–1094, <https://doi.org/10.1039/C5EE03165F>.
- [30] R. Lopez-Delgado, Y. Zhou, A. Zazueta-Raynaud, H. Zhao, J.E. Pelayo, A. Vomiero, M.E. Álvarez-Ramos, F. Rosei, A. Ayon, Enhanced conversion efficiency in Si solar cells employing photoluminescent down-shifting CdSe/CdS core/shell quantum dots, *Sci. Rep.* 7 (2017) 14104, <https://doi.org/10.1038/s41598-017-14269-0>.
- [31] N. Liu, H. Xue, Y. Ji, J. Wang, ZnSe/ZnS core-shell quantum dots incorporated with Ag nanoparticles as luminescent down-shifting layers to enhance the efficiency of Si solar cells, *J. Alloys Compd.* 747 (2018) 696–702, <https://doi.org/10.1016/j.jallcom.2018.03.060>.
- [32] S. Gardelis, A.G. Nassiopoulou, Evidence of significant down-conversion in a Si-based solar cell using CuInS₂/ZnS core shell quantum dots, *Appl. Phys. Lett.* 104 (2014) 183902, <https://doi.org/10.1063/1.4875616>.
- [33] M. Hong, T. Xuan, J. Liu, Z. Jiang, Y. Chen, X. Chen, H. Li, Air-exposing microwave-assisted synthesis of CuInS₂/ZnS quantum dots for silicon solar cells with enhanced photovoltaic performance, *RSC Adv.* 5 (2015) 102682–102688, <https://doi.org/10.1039/C5RA21454H>.
- [34] M. Jalalah, M.S. Al-Assiri, J.-G. Park, One-pot gram-scale, eco-friendly, and cost-effective synthesis of CuGaS₂/ZnS nanocrystals as efficient UV-harvesting down-

converter for photovoltaics, *Adv. Energy Mater.* 8 (2018) 1703418, <https://doi.org/10.1002/aenm.201703418>.

- [35] D. Hahm, J.H. Chang, B.G. Jeong, P. Park, J. Kim, S. Lee, J. Choi, W.D. Kim, S. Rhee, J. Lim, D.C. Lee, C. Lee, K. Char, W.K. Bae, Design principle for bright, robust, and color-pure InP/ZnSexS1-x/ZnS heterostructures, *Chem. Mater.* 31 (2019) 3476–3484, <https://doi.org/10.1021/acs.chemmater.9b00740>.
- [36] P.K. Nayak, S. Mahesh, H.J. Snaith, D. Cahen, Photovoltaic solar cell technologies: analysing the state of the art, *Nat. Rev. Mater.* 4 (2019) 269–285, <https://doi.org/10.1038/s41578-019-0097-0>.
- [37] V.I. Klimov, T.A. Baker, J. Lim, K.A. Velizhanin, H. McDaniel, Quality factor of luminescent solar concentrators and practical concentration limits attainable with semiconductor quantum dots, *ACS Photonics* 3 (2016) 1138–1148, <https://doi.org/10.1021/acsp Photonics.6b00307>.
- [38] M.G. Debije, P.P.C. Verbunt, Thirty years of luminescent solar concentrator research: solar energy for the built environment, *Adv. Energy Mater.* 2 (2012) 12–35, <https://doi.org/10.1002/aenm.201100554>.
- [39] I. Papakonstantinou, C. Tummelshammer, Fundamental limits of concentration in luminescent solar concentrators revised: the effect of reabsorption and nonunity quantum yield, *Optica* 2 (2015) 841–849, <https://doi.org/10.1364/OPTICA.2.000841>.
- [40] H.-J. Song, B.G. Jeong, J. Lim, D.C. Lee, W.K. Bae, V.I. Klimov, Performance limits of luminescent solar concentrators tested with seed/quantum-well quantum dots in a selective-reflector-based optical cavity, *Nano Lett.* 18 (2018) 395–404, <https://doi.org/10.1021/acs.nanolett.7b04263>.
- [41] A. Hassinen, I. Moreels, K. De Nolf, P.F. Smet, J.C. Martins, Z. Hens, Short-chain alcohols strip X-type ligands and quench the luminescence of PbSe and CdSe quantum dots, acetonitrile does not, *J. Am. Chem. Soc.* 134 (2012) 20705–20712, <https://doi.org/10.1021/ja308861d>.
- [42] D. Zherebetsky, M. Scheele, Y. Zhang, N. Bronstein, C. Thompson, D. Britt, M. Salmeron, P. Alivisatos, L.-W. Wang, Hydroxylation of the surface of PbS nanocrystals passivated with oleic acid, *Science* 344 (2014) 1380–1384, <https://doi.org/10.1126/science.1252727>.
- [43] H. Mattoussi, J.M. Mauro, E.R. Goldman, G.P. Anderson, V.C. Sundar, F. V. Mikulec, M.G. Bawendi, Self-assembly of CdSe–ZnS quantum dot bioconjugates using an engineered recombinant protein, *J. Am. Chem. Soc.* 122 (2000) 12142–12150, <https://doi.org/10.1021/ja002535y>.
- [44] F. Pinaud, D. King, H.-P. Moore, S. Weiss, Bioactivation and cell targeting of semiconductor CdSe/ZnS nanocrystals with phytochelatin-related peptides, *J. Am. Chem. Soc.* 126 (2004) 6115–6123, <https://doi.org/10.1021/ja031691c>.
- [45] H.T. Uyeda, L.L. Medintz, J.K. Jaiswal, S.M. Simon, H. Mattoussi, Synthesis of compact multidentate ligands to prepare stable hydrophilic quantum dot fluorophores, *J. Am. Chem. Soc.* 127 (2005) 3870–3878, <https://doi.org/10.1021/ja044031w>.
- [46] B.-K. Pong, B.L. Trout, J.-Y. Lee, Modified ligand-exchange for efficient solubilization of CdSe/ZnS quantum dots in water: a procedure guided by computational studies, *Langmuir* 24 (2008) 5270–5276, <https://doi.org/10.1021/la703431j>.
- [47] U. Ryde, Carboxylate binding modes in zinc proteins: a theoretical study, *Biophys. J.* 77 (1999) 2777–2787, [https://doi.org/10.1016/S0006-3495\(99\)77110-9](https://doi.org/10.1016/S0006-3495(99)77110-9).
- [48] A.R. Clapp, E.R. Goldman, H. Mattoussi, Capping of CdSe–ZnS quantum dots with DHLA and subsequent conjugation with proteins, *Nat. Protoc.* 1 (2006) 1258–1266, <https://doi.org/10.1038/nprot.2006.184>.
- [49] H. Takeuchi, B. Omogo, C.D. Heyes, Are bidentate ligands really better than monodentate ligands for nanoparticles? *Nano Lett.* 13 (2013) 4746–4752, <https://doi.org/10.1021/nl4023176>.
- [50] J. Lim, B.G. Jeong, M. Park, J.K. Kim, J.M. Pietryga, Y.-S. Park, V.I. Klimov, C. Lee, D.C. Lee, W.K. Bae, Influence of shell thickness on the performance of light-emitting devices based on CdSe/Zn1-XCdXS core/shell heterostructured quantum dots, *Adv. Mater.* 26 (2014) 8034–8040, <https://doi.org/10.1002/adma.201403620>.
- [51] A. Fokina, Y. Lee, J.H. Chang, M. Park, Y. Sung, W.K. Bae, K. Char, C. Lee, R. Zentel, The role of emission layer morphology on the enhanced performance of light-emitting diodes based on quantum dot-semiconducting polymer hybrids, *Adv. Mater. Interfaces* 3 (2016) 1600279, <https://doi.org/10.1002/admi.201600279>.



Donghyo Hahm received B.S. (2014) and Ph.D. (2020) in Chemical and Biological Engineering at Seoul National University (SNU) in Korea. He is currently a post-doctoral researcher at Sungkyunkwan University (SKKU). His interests include the synthesis and optical characterization of nanocrystal quantum dots.



Jeong Woo Park received his B.S. degree from Sungkyunkwan University (SKKU) in 2019. He is now a M.S. candidate in SKKU Advanced Institute of Nanotechnology (SAINT), Sungkyunkwan University. His research interests are the synthesis and optical analysis of colloidal quantum dots.



Jun Young Kim is an assistant professor at Department of Semiconductor Engineering, Gyeongsang National University (GNU). He received his Ph.D. degree from Seoul National University (SNU) in 2014. He was enrolled in Korea Institute of Industrial Technology (KITECH) as a senior researcher in 2016–2018 and LG Display as a senior researcher in 2014–2016 before he joined the faculty of GNU in 2018.



Hee-Eun Song received her Ph.D. in Chemistry at Washington University in MO, USA. After being a postdoc in Yale University, she joined Photovoltaic Laboratory at Korea Institute of Energy Research in 2010. Her main research field is dedicated to the thin Si wafer based photovoltaic cell and high performance photovoltaic cell structures.



Min Gu Kang is a principal researcher at the Photovoltaic Laboratory in Korea Institute of Energy Research, Daejeon, South Korea since 2012. He received his Ph.D. in Material Science from Korea University. His research interests include the development of highly efficient c-Si photovoltaic cell and its characterization method.



Byeong Guk Jeong received his Ph.D. degrees from Korea Advanced Institute of Science and Technology (KAIST), in 2019. He is now the post-doctoral researcher in SKKU Advanced Institute of Nanotechnology (SAINT), Sungkyunkwan University. His research interests are the synthesis of colloidal quantum dots and their optoelectronic applications.



Sohee Jeong is an associate professor in the Department of Energy Science in Sungkyunkwan University, South Korea. She was a principal researcher at Korea Institute of Machinery and Materials (KIMM) before she joined the faculty in SKKU. She received Ph.D. Chemistry degree from the University of Michigan in Ann Arbor, MI, USA.



Wan Ki Bae is an assistant professor at Department of Nano-Engineering and SAINT, Sungkyunkwan University. He received his Ph.D. degree from Seoul National University (SNU), South Korea in 2009. He was enrolled in Korea Institute of Science and Technology (KIST) as a senior researcher in 2013–2018 before he joined the faculty of SKKU in 2018.



Gihwan Kang received his Ph.D in Electrical engineering at Konkuk University. He is currently a president of the Korean Solar Energy Society and a director of Korean Photovoltaic Society. Also, he is a principal researcher in Photovoltaic Laboratory, Korea Institute of Energy Research. Since 1987, he has been focused on highly efficient c-Si photovoltaic module and building integrated photovoltaic systems.



Hyung-Jun Song received his Ph.D in Electrical engineering at Seoul National University in 2015. After a postdoctoral training at Los Alamos National Laboratory (NM, USA), he is an assistant professor at Department of Safety Engineering in Seoul National University of Science and Technology, Seoul, South Korea. His current research is focused on the developing highly efficient and reliable photovoltaic module and system.